

Layer-skipping connections facilitate training of layered networks using equilibrium propagation.

Jimmy Gammell^{1,*}, Sonia Buckley¹, Sae Woo Nam¹ and Adam N. McCaughan¹

¹ National Institute of Standards and Technology, Boulder, CO, United States

Correspondence*:

Jimmy Gammell

jimmy.gammell@colorado.edu

2 ABSTRACT

3 Equilibrium propagation is a learning framework that marks a step forward in the search for a
4 biologically-plausible implementation of deep learning, and could be implemented efficiently in
5 neuromorphic hardware. Previous applications of this framework to layered networks encountered
6 a vanishing gradient problem that has not yet been solved in a simple, biologically-plausible way.
7 In this paper, we demonstrate that the vanishing gradient problem can be mitigated by replacing
8 some of a layered network's connections with random layer-skipping connections. We additionally
9 analyze the notion of "biological plausibility" by comparing the computational requirements of
10 equilibrium propagation to those of the more conventional backpropagation algorithm, and find
11 that (FIXME conclusion?).

12 **Keywords:** equilibrium propagation, deep learning, small-world, layer-skipping connections, neuromorphic computing, biologically-
13 motivated

14 **Number of words:** 5137

15 **Number of figures:** 7

16 **Number of tables:** 1

1 INTRODUCTION

17 As research into neural networks grows, there has been increased interest in designing biologically-inspired
18 training algorithms, as they may offer insight into biological learning processes and also offer clues towards
19 developing energy-efficient neuromorphic systems [FIXME find a reference for this statement]. The equi-
20 librium propagation learning framework developed Scellier and Bengio [2016] is one such algorithm. It is a
21 method for training a class of energy-based networks, the prototype for which is the continuous Hopfield netw-
22 ork Hopfield [1984]. In particular, it addresses one of the major issues that prevent other training algorithms
23 (such as backpropagation) from being biologically-plausible, such as using separate computation pathways
24 for different phases of training. This feature also makes the algorithm appealing for practical implementation
25 into neuromorphic hardware, because only a single computation circuit is required within the neuron, rather

than multiple distinct circuits. However, current implementations of the algorithm still have a defect that diminishes its biological plausibility: they require hand-tuned per-layer hyperparameters to account for a vanishing gradient through the network. In addition to not being biologically plausible, these multiplicative hyperparameters would be difficult to implement in a neuromorphic hardware system with limited bit depth. In this work, we demonstrate that the vanishing gradient problem can instead be solved through topological means: by randomly replacing some of a layered network’s connections with layer-skipping connections, we can generate a small-world network that trains each layer more evenly and does not need per-layer hyperparameters.

Implementation of equilibrium propagation in [Scellier and Bengio, 2016] was hindered by a vanishing gradient problem whereby networks with as few as 3 hidden layers trained slowly on MNIST [LeCun and Cortes, 1998] – a serious issue given that network depth is critical to performance on difficult datasets [Simonyan and Zisserman, 2014; Srivastava et al., 2015b] and that convergence to a low error rate on MNIST is a low bar to meet. The problem was overcome in [Scellier and Bengio, 2016] by independently tuning a unique learning rate for each layer in the network. These learning rates were multiplicative factors that proportionally scaled the signals communicated between layers.

In our work, we have modified the strictly-layered topology of the original implementation by adding and removing connections to create a small-world network [Watts and Strogatz, 1998]. Through this modification we have eliminated the per-layer hyperparameters without degrading the algorithm’s performance – the modified network produces 0% training error (out of 50,000 examples) and $\lesssim 2.5\%$ test error (out of 10,000 examples) on MNIST using a network with three hidden layers and no regularization term in its cost function. These error rates are comparable to those of other biologically-motivated networks [Bartunov et al., 2018] and are approximately the same as those of the layered network with unique, manually-tuned learning rates in [Scellier and Bengio, 2016]. Our method could be implemented with relative ease in any system with configurable connectivity, such as those already described in several neuromorphic hardware platforms [FIXME cite loihi, brainscales, <https://aip.scitation.org/doi/abs/10.1063/1.5096403>]. Layer-skipping connections have been observed in biological brains [Bullmore and Sporns, 2009], so the approach is biologically-plausible. Similar techniques have seen success in convolutional [He et al., 2015; Srivastava et al., 2015a] and multilayer feedforward [Xiaohu et al., 2011; Krishnan et al., 2019] networks. Our findings outlined in this paper suggest that layer-skipping connections are effective-enough to be appealing in contexts where simplicity and biological plausibility are important.

2 BACKGROUND

2.1 Equilibrium propagation

Similar to backpropagation, the equilibrium propagation algorithm [Scellier and Bengio, 2016] trains networks by approximating gradient descent on a cost function. Equilibrium propagation is applicable to any network with dynamics characterized by evolution to a fixed point of an associated energy function; our implementation is a recreation of that in [Scellier and Bengio, 2016], which applies it to a continuous Hopfield network [Hopfield, 1984]. The mathematical formulation of the framework can be found in [Scellier and Bengio, 2016]. We discuss its appeal relative to backpropagation in section 5.1.

2.1.1 Implementation in a continuous Hopfield network

Here we summarize the equations through which a continuous Hopfield network is trained using equilibrium propagation; this summary is based on the more-thorough and more-general treatment in [Scellier and Bengio, 2016].

Consider a network with n neurons organized into an input layer with p neurons, hidden layers with q neurons and an output layer with r neurons. Let the activations of these neurons be denoted respectively

by vectors $\mathbf{x} \in \mathbb{R}^p$, $\mathbf{h} \in \mathbb{R}^q$ and $\mathbf{y} \in \mathbb{R}^r$, and let $\mathbf{s} = (\mathbf{h}^T, \mathbf{y}^T)^T \in \mathbb{R}^{q+r}$ and $\mathbf{u} = (\mathbf{x}^T, \mathbf{s}^T)^T \in \mathbb{R}^n$ be vectors of, respectively, the activations of non-fixed (non-input) neurons and of all neurons in the network. Let $\mathbf{W} \in \mathbb{R}^{n \times n}$ and $\mathbf{b} \in \mathbb{R}^n$ denote the network's weights and biases where w_{ij} is the connection weight between neurons i and j and b_i is the bias for neuron i ($\forall i, w_{ii} = 0$ to prevent self-connections), and let ρ denote its activation function; here and in [Scellier and Bengio, 2016],

$$\rho(x) = \begin{cases} 0 & x < 0 \\ x & 0 \leq x \leq 1 \\ 1 & x > 1 \end{cases} \quad (1)$$

is a hardened sigmoid function where $\rho'(0) = \rho'(1)$ is defined to be 1 to avoid neuron saturation. Let $\rho((x_1, \dots, x_n)^T) = (\rho(x_1), \dots, \rho(x_n))^T$.

The behavior of the network is to perform gradient descent on a total energy function F that is modified by a training example $(\mathbf{x}_d, \mathbf{y}_d)$. Consider energy function $E: \mathbb{R}^n \rightarrow \mathbb{R}$,

$$E(\mathbf{u}; \mathbf{W}, \mathbf{b}) = \frac{1}{2} \mathbf{u}^T \mathbf{u} - \frac{1}{2} \rho(\mathbf{u})^T \mathbf{W} \rho(\mathbf{u}) - \mathbf{b}^T \mathbf{u} \quad (2)$$

and arbitrary cost function $C: \mathbb{R}^r \rightarrow \mathbb{R}_+$; here and in [Scellier and Bengio, 2016] it is a quadratic cost function given by

$$C(\mathbf{y}) = \frac{1}{2} \|\mathbf{y} - \mathbf{y}_d\|_2^2, \quad (3)$$

though the framework still works for cost functions incorporating a regularization term dependent on \mathbf{W} and \mathbf{b} . The total energy function $F: \mathbb{R}^n \rightarrow \mathbb{R}$ is given by

$$F(\mathbf{u}; \beta, \mathbf{W}, \mathbf{b}) = E(\mathbf{u}; \mathbf{W}, \mathbf{b}) + \beta C(\mathbf{y}) \quad (4)$$

where the clamping factor β is a small constant. \mathbf{s} evolves over time t as

$$\frac{d\mathbf{s}}{dt} \propto -\frac{\partial F}{\partial \mathbf{s}}. \quad (5)$$

Equilibrium has been reached when $\frac{\partial F}{\partial \mathbf{s}} \approx 0$. This can be viewed as solving the optimization problem

$$\underset{\mathbf{s} \in \mathbb{R}^{q+r}}{\text{minimize}} F((\mathbf{x}_d^T, \mathbf{s}^T)^T; \beta, \mathbf{W}, \mathbf{b}) \quad (6)$$

by using gradient descent to find a local minimum of F .

The procedure for training on a single input-output pair $(\mathbf{x}_d, \mathbf{y}_d)$ is as follows:

1. Clamp \mathbf{x} to \mathbf{x}_d and perform the free-phase evolution: evolve to equilibrium on the energy function $F(\mathbf{u}; 0, \mathbf{W}, \mathbf{b})$ in a manner dictated by equation 5. Record the equilibrium state \mathbf{u}^0 .
2. Perform the weakly-clamped evolution: evolve to equilibrium on the energy function $F(\mathbf{u}; \beta, \mathbf{W}, \mathbf{b})$ using \mathbf{u}^0 as a starting point. Record the equilibrium state \mathbf{u}^β .
3. Compute the correction to each weight in the network:

$$\Delta W_{ij} = \frac{1}{\beta} (\rho(u_i^\beta) \rho(u_j^\beta) - \rho(u_i^0) \rho(u_j^0)). \quad (7)$$

90 Adjust the weights using $W_{ij} \leftarrow W_{ij} + \alpha \Delta W_{ij}$ where the learning rate α is a positive constant.

91 4. Compute the correction to each bias in the network:

$$\Delta b_i = \frac{1}{\beta} (\rho(u_i^\beta) - \rho(u_i^0)) \quad (8)$$

92 and adjust the biases using $b_i \leftarrow b_i + \alpha \Delta b_i$.

93 This can be repeated on as many training examples as desired. Training can be done on batches by computing
 94 ΔW_{ij} and Δb_i for each input-output pair in the batch, and correcting using the averages of these values. Note
 95 that the correction to a weight is computed using only the activations of neurons it directly affects, and the
 96 correction to a bias is computed using only the activation of the neuron it directly affects. This contrasts
 97 with backpropagation, where to correct a weight or bias l layers from the output it is necessary to know the
 98 activations, derivatives and weights of all neurons between 0 and $l - 1$ layers from the output.

99 2.2 Vanishing gradient problem

100 Vanishing gradients are problematic because they reduce a network’s rate of training and could be difficult to
 101 represent in neuromorphic analog hardware due to limited bit depth. As a simple example, the multiplicative
 102 factor of 0.008 used in previous implementations would lead to significant precision errors in a system with
 103 signals represented by integers from 0-16 (bit depth of 4).

104 The vanishing gradient problem is familiar in the context of conventional feedforward networks, where
 105 techniques such as the weight initialization scheme in [Glorot and Bengio, 2010], the use of activation
 106 functions with derivatives that do not lead to output saturation [Schmidhuber, 2015], and batch normalization
 107 [Ioffe and Szegedy, 2015] have been effective at overcoming it. However, in the context of the networks
 108 trained in [Scellier and Bengio, 2016], the vanishing gradient problem persists even when the former two
 109 techniques are used. To our knowledge batch normalization has not been used in the context of equilibrium
 110 propagation; however, it seems unlikely to be biologically-plausible.

3 IMPLEMENTATION

We recreated the equilibrium propagation implementation¹ in [Scellier and Bengio, 2016] using the Pytorch library. Like the networks in [Scellier and Bengio, 2016], our networks are continuous Hopfield networks with a hardened sigmoid activation function

$$\sigma(x) = \text{Max}\{0, \text{Min}\{x, 1\}\}$$

and squared-error cost function with no regularization term

$$C = ||\mathbf{y} - \mathbf{y}_d||_2^2,$$

111 where \mathbf{y} is the network’s output and \mathbf{y}_d is the target output. Tests were run on MNIST [LeCun and Cortes,
 112 1998] grouped into batches of 20 examples, with the 50,000 training examples used for training and the
 113 10,000 validation examples used for computing test errors.

114 We use two performance-enhancing techniques that were used in [Scellier and Bengio, 2016]: we random-
 115 ize the sign of β before training on each batch, which has a regularization effect, and we use persistent
 116 particles, where the state of the network after training on a given batch during epoch n is used as the initial

¹ https://github.com/jgammell/Equilibrium_Propagation_mobile.git

state for that batch during epoch $n + 1$. Persistent particles reduce the computational resources needed to approximate the differential equation governing network evolution, and would be unnecessary in an analog implementation that can approximate the equation efficiently. Note that this technique leads to higher error rates early in training than would be present with a more-thorough approximation of the differential equation.

3.1 Layered topology with per-layer rates

We recreated the 5-layer network evaluated in [Scellier and Bengio, 2016]. It has the standard layered topology shown in figure 1, and consists of a 784-neuron input layer, 3 500-neuron hidden layers and a 10-neuron output layer. Weights are initialized using the scheme from [Glorot and Bengio, 2010]. As mentioned above, each layer has a unique learning rate; the rates are $\alpha_1 = .128$, $\alpha_2 = .032$, $\alpha_3 = .008$ and $\alpha_4 = .002$ where α_i is the learning rate for the connection weights between layers i and $i + 1$ and for the biases in layer i , and the input and output layers are denoted $i = 1$ and $i = 5$, respectively.

3.2 Layered topology with global learning rate

To illustrate the vanishing gradient problem and provide a point of reference, we also tested the network

3.3 Our topology

in section 3.1 with a single global learning rate of .02.

Algorithm 1: Algorithm to produce our topology

Input: Layered network from section 3.2

Input: Integer n , giving number of connections to replace

Output: A network with our modified topology

for hidden layer in network **do**

 Add edge between each pair of neurons in layer

for $i \leftarrow 1$ **to** n **do**

 Randomly select pre-existing connection in network;

 Add connection between random unconnected pair of neurons in network;

 // Do not allow self connections

 // Do not allow connections

 between two input neurons or between two output neurons

 Remove pre-existing connection;

return modified network

To generate a network with our topology, we use algorithm 1. This topology is illustrated in figure 2. The above algorithm is approximately equivalent to the algorithm for generating a small-world network described in [Watts and Strogatz, 1998] with $p = 1 - (\frac{N_o - 1}{N_o})^n$ for $p \lesssim .2$, where N_o is the number of connections in the network; to contextualize the number of replaced connections we will henceforth describe networks with our topology in terms of p instead of n . We have seen good results with $p \approx 8\%$. We have seen similar results when connections are added to the network, rather than randomly replaced (algorithm 1, without removing pre-existing connections).

For these networks we use a global learning rate of .02 and, as in the networks from sections 3.1 and 3.2, initialize connections between neurons in adjacent layers using the scheme from [Glorot and Bengio, 2010]. For all other connections we draw initial weights from the uniform distribution $U[-.05, .05]$ where the value .05 was determined empirically to yield good results.

4 RESULTS

We compared the networks described in section 3 by observing their behavior while training on MNIST [LeCun and Cortes, 1998]. All networks used $\epsilon = .5$, $\beta = 1.0$, 500 free-phase iterations, 8 weakly-distributed connections, and were trained for 250 epochs.

Figure 3 illustrates that our network significantly outperforms one with a global learning rate, and achieves close to the same training and test error rates as one with unique learning rates, albeit after around 25% more epochs. Both our network and the layered network with unique learning rates achieve approximately a 2.5% test error and 0% training error, whereas the layered network with a global learning rate has test and training error rates of 6% and 10% respectively.

To observe the extent of the vanishing gradient problem, for each network we tracked the root-mean-square correction to weights in each of its layers during training on MNIST [LeCun and Cortes, 1998]. Figure 4 shows an 11-point centered moving average of these values (without averaging the values are very volatile). It can be seen that for the layered network with a global learning rate, the magnitude of the correction to a typical neuron vanishes with depth relative to the output, with the shallowest weights training around 100 times faster than the deepest weights - this illustrates the vanishing gradient problem. The use of unique learning rates is very effective at making corrections uniform. Our topology with $p = 7.56\%$ is effective at making deeper layers train in a uniform way, but the output layer still trains around 10 times faster than deeper layers; nonetheless, figure 3 suggests that this imperfect solution still yields a significant performance benefit.

The fast training of the output layer in the network with our topology is probably because no layer-skipping connections attach directly to the target output, so for any value of p the shortest path between a deep neuron and the target layer is at least 2 connections long, whereas the path between an output neuron and the target layer is 1 connection long.

We tracked the training error after one epoch of a network with our topology while varying p ; the results are shown in figure 5. For $p < .1\%$, there is little improvement in the error rate as p is increased, but there is substantial improvement in the uniformity of the training rates of deep layers. When $p > .1\%$, the deep layers are very uniform, and the error rate starts decreasing with p at a rate that is slightly slower than exponential; at this point there is little improvement in the uniformity of deep layers, but the rate of the shallowest layer appears to move closer to those of the deeper layers.

We found that our topology performs significantly worse than the basic topology with one learning rate when few connections are replaced. This could be due to a poor weight initialization scheme for the added intralayer connections; we have noticed anecdotally that networks appear to be less-sensitive to their weight initialization scheme as connections are replaced. We have found that networks perform poorly relative to a basic network with one learning rate until p is in the ballpark of 7%. This experiment suggests that training rate will keep improving long after that, but does not show long-term performance or test performance; we suspect that a network’s generalization ability will suffer for large p as it loses its regimented nature.

5 DISCUSSION

5.1 Comparing

the computational complexity of equilibrium propagation and backpropagation

182 The main motivations for using equilibrium propagation instead of an alternative machine learning
 183 technique (such as deep learning using backpropagation for training) are 1) to gain insight into the operation
 184 of the brain by developing target-based learning approaches in biologically plausible networks and 2) to
 185 develop algorithms that are more easily implemented in hardware. Below we qualitatively compare the
 186 hardware that would be needed for implementation of equilibrium propagation versus for backpropagation
 187 on a standard feedforward network to gain insight into the utility of these networks.

188 5.1.1 Requirements of equilibrium propagation

Just as in the algorithm, to implement equilibrium propagation in hardware, three different phases of hardware operation are required. In the first (free running) phase, it follows from equations 2, 4 and 5 that to determine its state, the i -th neuron in a network must compute

$$\frac{\partial F}{\partial u_i} = u_i - \frac{1}{2} \rho'(u_i) \left[\sum_{i \neq j} W_{ij} \rho(u_j) + b_i \right],$$

189 plus the term $\beta(u_i - y_i^{target})$ for output neurons when using a squared-error cost function, and then integrate
 190 the result over time. Parameter correction rules are given by equations 7 and 8. This is exactly the operation
 191 of an analog leaky integrate and fire neuron, as for example implemented in the neuromorphic hardware
 192 platforms of Refs. ?? among others. A qualitative diagram of potential neuron and synapse devices and their
 193 output and read/write to memory operations are shown in the diagram in Fig. ?? (a). At each neuron N_i^l the
 194 value of $U_{i,0}^{l+1}$ is written to memory and the nonlinear function ρ is applied before sending to the synapse
 195 device, where it is multiplied by the weight w_{ij}^{l+1} which is read from memory by the synapse device. These
 196 weighted outputs are summed at the input of the next neuron device (N_j^{l+1}) and added to a bias value b_j^{l+1}
 197 that is read from memory to generate U_{l+1} . A block diagram showing the same thing in more detail is shown
 198 in the Appendix.

199 In the second (weakly-clamped) phase, shown in Fig. ?? (b), the operation of the hardware is exactly the
 200 same as in (a), with the value U_β written to memory at each neuron. Not shown in Fig. 6 is the functionality
 201 at the output neurons which are weakly clamped and have a new function in this phase, this is shown in Fig.
 202 X in the Appendix.

203 Finally, in the third phase, the weights and biases are updated as shown in Fig. ?? (c). At each neuron
 204 device the values of U_0 and U_β are read from memory and $\rho(U_0)$ and $\rho(U_\beta)$ are calculated. At the synapse
 205 device, the computation of Eq. X is performed using these values from the pre- and post- synaptic neurons
 206 to calculate the weight update Δw , and the value of the weight in memory is updated to $w + \Delta w$. Similar
 207 updates are applied to the bias b at every neuron according to Eq. Y. Brief sentence on number of neurons
 208 versus synapses for the read/write to memory operations.

209 5.1.2 Requirements of backpropagation

Backpropagation is an algorithm for training networks using gradient descent. It is most typically applied to feedforward neural networks, in which the activation value of a neuron i in layer l is given by

$$\rho(u_i^l) = \rho\left(\sum_j W_{ij}^l u_j^{l-1} + b_i^l\right).$$

This is very similar to the free running situation in equilibrium propagation, with the main difference being that the connections are unidirectional. The qualitative implementation of this inference phase in hardware is shown in Fig. ?? (a). Using backpropagation, the parameters are then updated by computing error correction

terms δ_i^l for each neuron i in layer l ; for the output layer L the correction is

$$\delta_i^L = \rho'(u_i^L)(\rho(u_i^L) - y_i^{target})$$

and for deeper layers it is

$$\delta_i^l = \rho'(u_i^l) \sum_j W_{ij}^{l+1} \delta_j^{l+1}.$$

The implementation of this in hardware is shown in Fig. ?? (b) (excluding layer L). Note that the data is now moving in the opposite (backwards) direction, and unlike in the case of equilibrium propagation, the functions implemented by the neurons are entirely different to the operation in the forward phase shown in (a). In a final phase, weights are corrected using

$$\Delta W_{ij}^l = \rho(u_i^{l-1}) \delta_j^l$$

and biases using

$$\Delta b_i^l = \delta_i^l.$$

210 This is shown in Fig. ?? (c).

211 5.1.3 Comparison

212 The most-significant difference between the algorithms is that in equilibrium propagation, the free and
 213 weakly-clamped phases of training are identical for most neurons and the weakly-clamped phase requires
 214 only slight modification to output neurons, whereas in backpropagation these phases very different functiona-
 215 lity from essentially all neurons. not sure I understand this next sentence Another visible difference is that in
 216 equilibrium propagation each neuron corresponds to a single synapse whereas in backpropagation a neuron
 217 corresponds to two synapses; we do not expect this difference to be significant because a synapse in the
 218 former case a synapse takes as inputs the outputs of all neighboring neurons, whereas in the latter case each
 219 has inputs from either shallower or deeper neurons (about half as many). Neurons in equilibrium propagation
 220 explicitly write their states to memory after the free and weakly-clamped phases, and therefore it requires the
 221 same amount of memory as for backpropagation. In backpropagation, distinct state variables are needed to
 222 hold the activation and error term of each neuron. For a hardware implementation, the need for distinct free
 223 and weakly-clamped phases (temporally non-local credit assignment) significantly reduces the advantages
 224 associated with the spatially local credit assignment. Recently there has been new work that indicates that
 225 the algorithm can be modified to eliminate the need for both phases ?. This would significantly reduce the
 226 memory requirements of the algorithm. Various characteristics of both algorithms are compared side-by-side
 227 in table 1. We should also discuss the layer skipping connections with respect to the implementation of this
 228 algorithm in hardware - just a sentence about it

229 5.2 Related work

230 References [Lee et al., 2015; Xie and Seung, 2003; Pineda, 1987] describe other approaches to locally
 231 approximating the gradient of a cost function. References [Lillicrap et al., 2014; Crafton et al., 2019] explore
 232 the use of a random feedback matrix for backwards connections that is more biologically-plausible than
 233 identical forwards and backwards connections. Reference [Bartunov et al., 2018] explores the present state of
 234 biologically-motivated deep learning, and [Bengio et al., 2015] discusses the criteria a biologically-plausible
 235 network would need to satisfy. References [Shainline et al., 2019; Davies et al., 2018; Nahmias et al., 2013]
 236 discuss analog hardware that could potentially implement equilibrium propagation. References [He et al.,
 237 2015; Srivastava et al., 2015a; Xiaohu et al., 2011; Krishnan et al., 2019] use layer-skipping connections for

other types of networks and learning frameworks. References [Ioffe and Szegedy, 2015; Glorot and Bengio, 2010] give approaches to solving vanishing gradient problems.

5.3 Directions for Future Research

There are several directions in which future research could be taken:

- Evaluating the effectiveness of this approach on hard datasets, such as CIFAR and ImageNet.
- Evaluating the effect of p on a network's test error.
- Exploring the effectiveness of layer-skipping connections on deeper networks.
- Exploring the effectiveness of a network when layer-skipping connections are used during training and removed afterwards.

CONFLICT OF INTEREST STATEMENT

The authors declare that the research was conducted in the absence of any commercial or financial relationships that could be construed as a potential conflict of interest.

The U.S. Government is authorized to reproduce and distribute reprints for governmental purposes notwithstanding any copyright annotation thereon.

REFERENCES

- Bartunov, S., Santoro, A., Richards, B. A., Hinton, G. E., and Lillicrap, T. P. (2018). Assessing the scalability of biologically-motivated deep learning algorithms and architectures. *CoRR* abs/1807.04587
- Bengio, Y., Lee, D., Bornschein, J., and Lin, Z. (2015). Towards biologically plausible deep learning. *CoRR* abs/1502.04156
- Bullmore, E. and Sporns, O. (2009). Complex brain networks: graph theoretical analysis of structural and functional systems. *Nature*
- Crafton, B., Parihar, A., Gebhardt, E., and Raychowdhury, A. (2019). Direct feedback alignment with sparse connections for local learning. *CoRR* abs/1903.02083
- Davies, M., Srinivasa, N., Lin, T.-H., Chinya, G., Joshi, P., Lines, A., et al. (2018). Loihi: A neuromorphic manycore processor with on-chip learning. *IEEE Micro* PP, 1–1. doi:10.1109/MM.2018.112130359
- Glorot, X. and Bengio, Y. (2010). Understanding the difficulty of training deep feedforward neural networks. In *Proceedings of the Thirteenth International Conference on Artificial Intelligence and Statistics*, eds. Y. W. Teh and M. Titterton (Chia Laguna Resort, Sardinia, Italy: PMLR), vol. 9 of *Proceedings of Machine Learning Research*, 249–256
- He, K., Zhang, X., Ren, S., and Sun, J. (2015). Deep residual learning for image recognition. *CoRR* abs/1512.03385
- Hopfield, J. (1984). Neurons with graded response have collective computational properties like those of two-state neurons. *Proceedings of the National Academy of Sciences of the United States of America* 81, 3088–92. doi:10.1073/pnas.81.10.3088
- Ioffe, S. and Szegedy, C. (2015). Batch normalization: Accelerating deep network training by reducing internal covariate shift. *CoRR* abs/1502.03167
- Krishnan, G., Du, X., and Cao, Y. (2019). Structural pruning in deep neural networks: A small-world approach
- [Dataset] LeCun, Y. and Cortes, C. (1998). The mnist database of handwritten digits
- Lee, D.-H., Zhang, S., Fischer, A., and Bengio, Y. (2015). Difference target propagation. 498–515. doi:10.1007/978-3-319-23528-8_31

- 277 Lillicrap, T. P., Cownden, D., Tweed, D. B., and Akerman, C. J. (2014). Random feedback weights support
278 learning in deep neural networks
- 279 Nahmias, M., Shastri, B., Tait, A., and Prucnal, P. (2013). A leaky integrate-and-fire laser neuron for
280 ultrafast cognitive computing. *Selected Topics in Quantum Electronics, IEEE Journal of* 19, 1–12.
281 doi:10.1109/JSTQE.2013.2257700
- 282 Pineda, F. (1987). Generalization of back-propagation to recurrent neural networks. *Physical Review Letters*
283 59, 2229–2232
- 284 Scellier, B. and Bengio, Y. (2016). Equilibrium propagation: Bridging the gap between energy-based models
285 and backpropagation
- 286 Schmidhuber, J. (2015). Deep learning in neural networks: An overview. *Neural Networks* 61, 85–117.
287 doi:10.1016/j.neunet.2014.09.003
- 288 Shainline, J. M., Buckley, S. M., McCaughan, A. N., Chiles, J. T., Jafari Salim, A., Castellanos-Beltran,
289 M., et al. (2019). Superconducting optoelectronic loop neurons. *Journal of Applied Physics* 126, 044902.
290 doi:10.1063/1.5096403
- 291 Simonyan, K. and Zisserman, A. (2014). Very deep convolutional networks for large-scale image recognition
- 292 Srivastava, R. K., Greff, K., and Schmidhuber, J. (2015a). Highway networks. *CoRR* abs/1505.00387
- 293 Srivastava, R. K., Greff, K., and Schmidhuber, J. (2015b). Training very deep networks
- 294 Watts, D. and Strogatz, S. (1998). Collective dynamics of 'small-world' networks. *Nature*
- 295 Xiaohu, L., Xiaoling, L., Jinhua, Z., Yulin, Z., and Maolin, L. (2011). A new multilayer feedforward
296 small-world neural network with its performances on function approximation. In *2011 IEEE International*
297 *Conference on Computer Science and Automation Engineering*
- 298 Xie, X. and Seung, H. (2003). Equivalence of backpropagation and contrastive hebbian learning in a layered
299 network. *Neural computation* 15, 441–54. doi:10.1162/089976603762552988

FIGURES

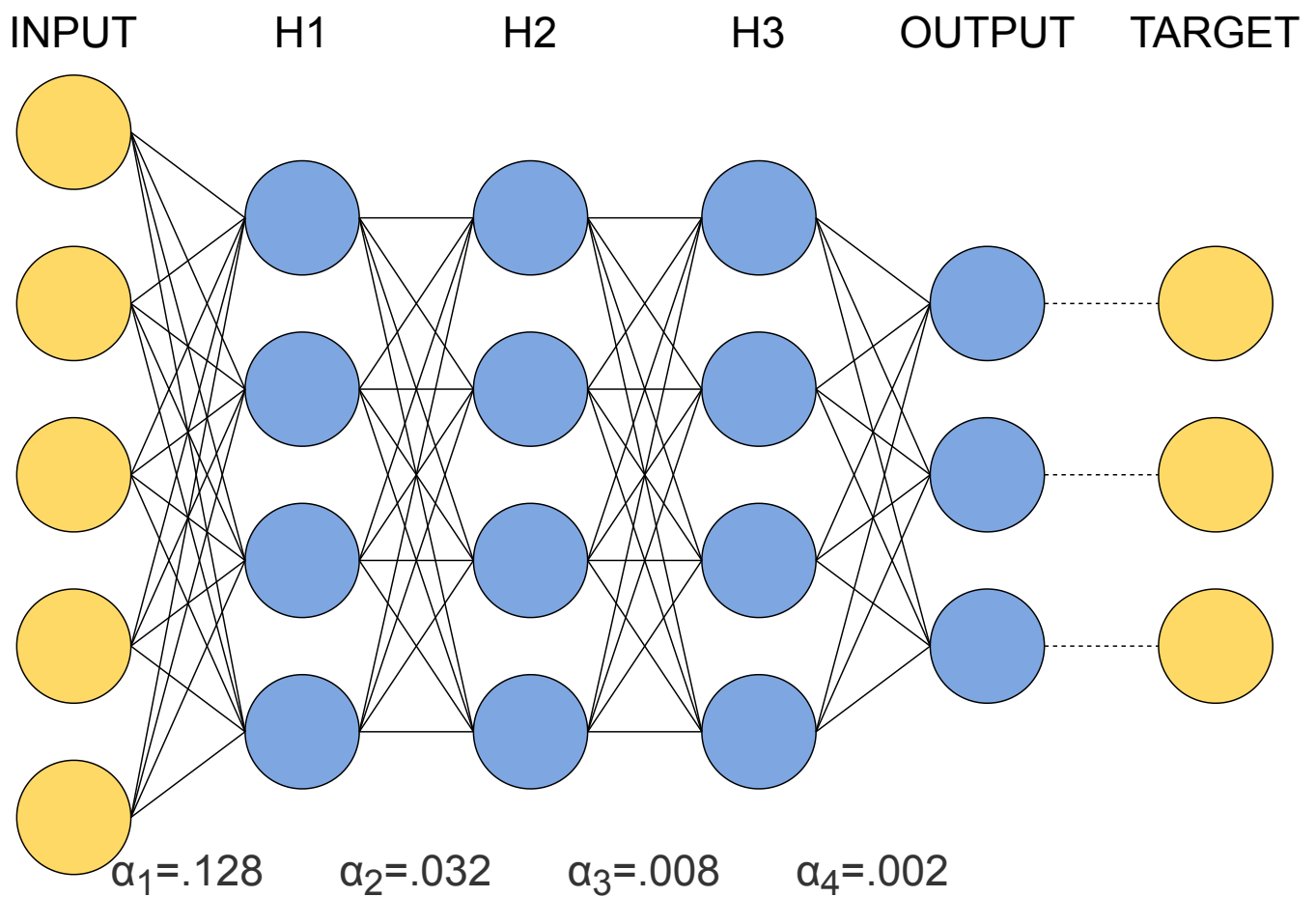


Figure 1. Topology of the layered network tested in [Scellier and Bengio, 2016]. All pairs of neurons in adjacent layers are connected. All connections are bidirectional. To compensate for the vanishing gradient problem, the learning rate is reduced by a factor of 4 each time distance from the output decreases by one layer.

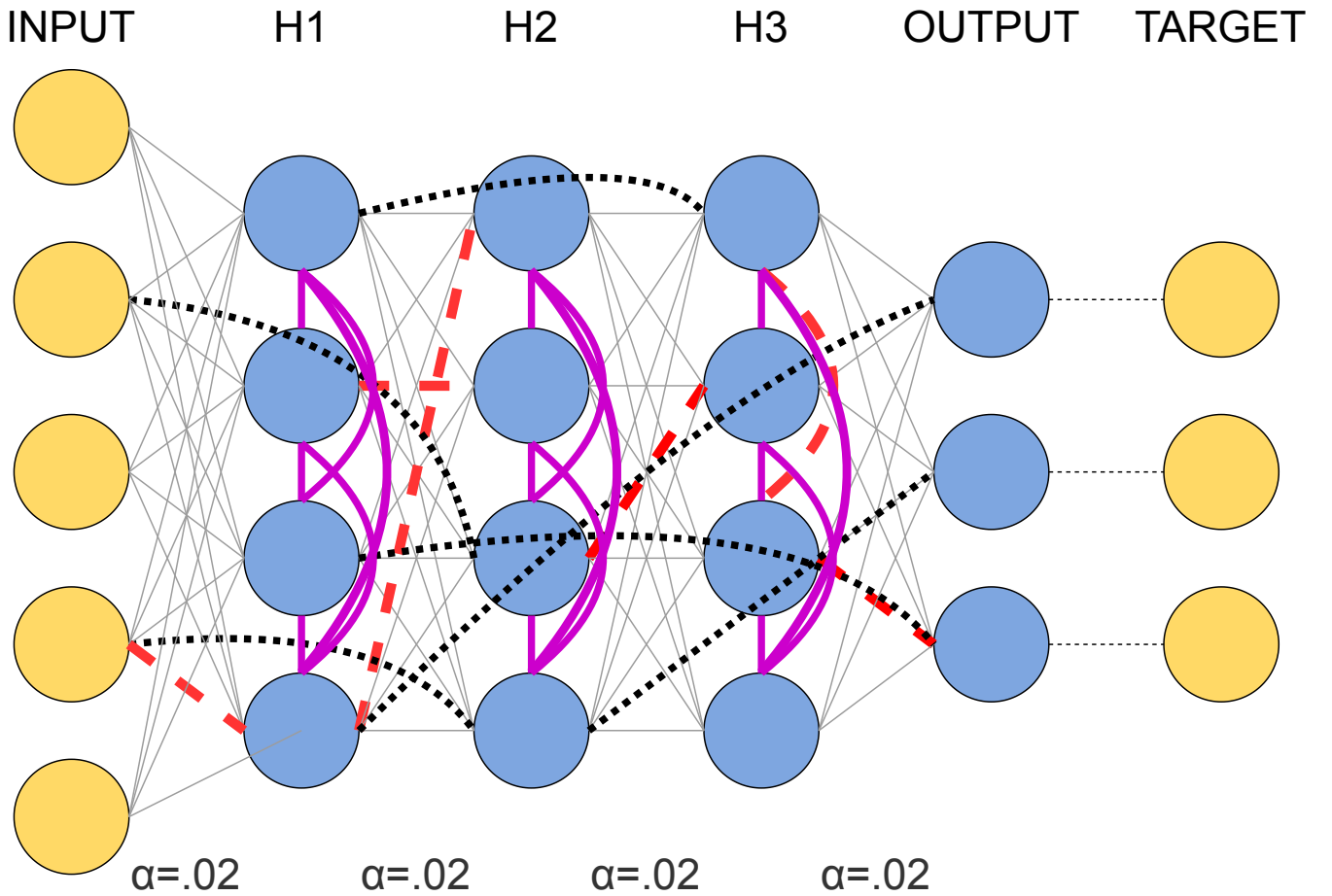


Figure 2. Our modifications to the topology of figure 1 to avoid a vanishing gradient while using a global learning rate. Red dotted lines denote connections that have been removed, black dotted lines denote their replacements, and green solid lines denote added intralayer connections. All connections are bidirectional. This illustration shows a network with $p = 8\%$.

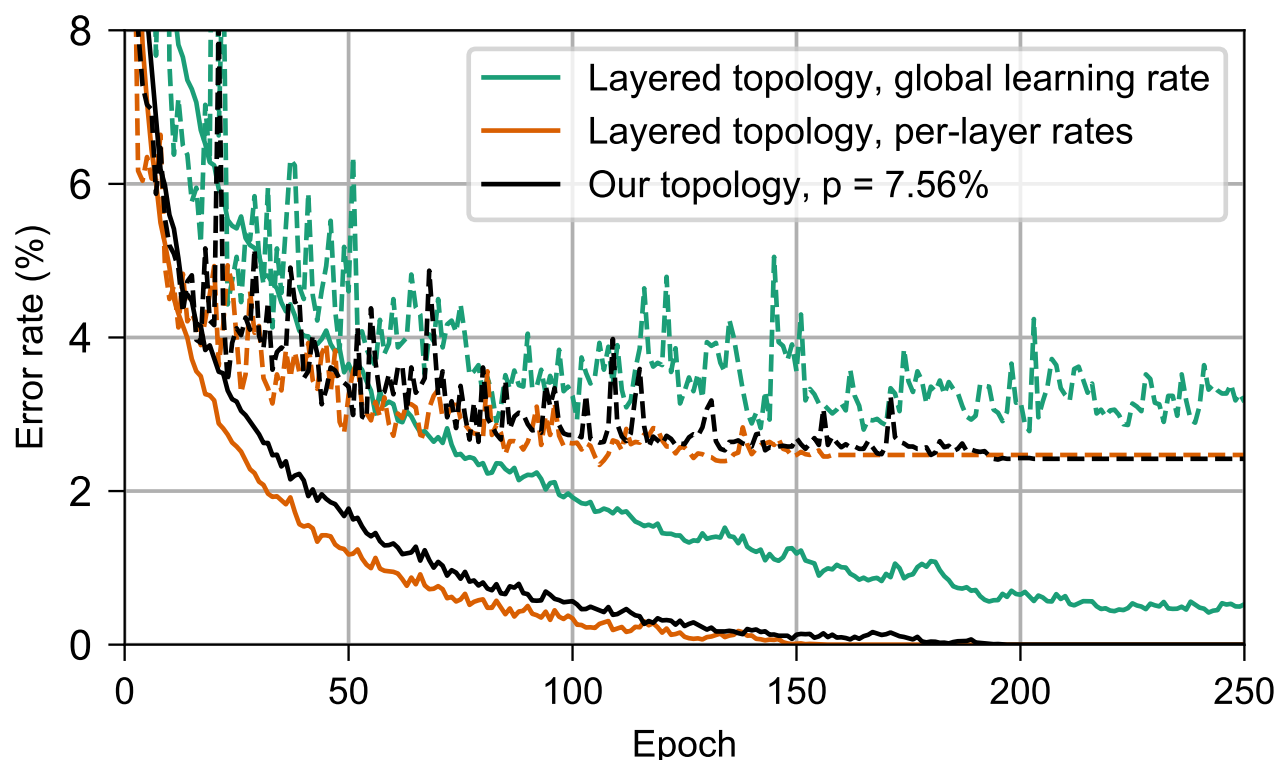


Figure 3. Performance on MNIST of the networks in section 3. Dashed lines show the test error and solid lines show the training error. In green is a layered network with a global learning rate (section 3.2), in orange is a layered network with per-layer rates individually tuned to counter the vanishing gradient problem (section 3.1), and in green is a network with our topology, $p = 7.56\%$ (section 3.3). Observe that our topology is almost as effective as per-layer rates at countering the vanishing gradient problem that impedes training of the layered network with a global learning rate.

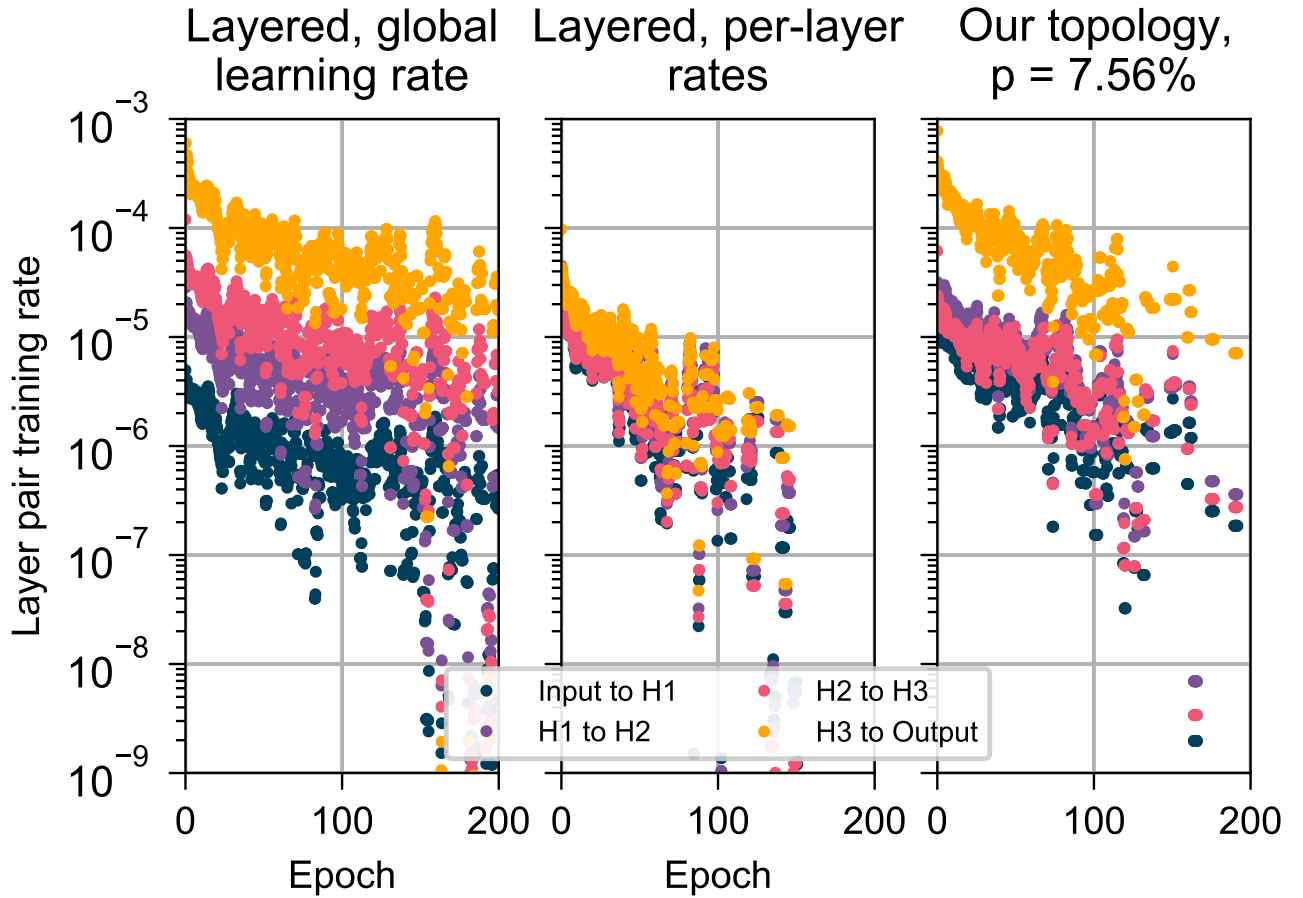


Figure 4. Root-mean-square corrections to weights in different layers while training on MNIST, for the networks in section 3. For clarity, values were subjected to an 11-point centered moving average. (left) A layered network with a single global learning rate (section 3.2). (center) A layered network a unique, individually-tuned learning rate for each layer (section 3.1). (right) A network with our topology, $p = 7.56\%$ (section 3.3). Observe that the layered topology with a global learning rate has a vanishing gradient problem, which is almost completely solved by tuning an individual learning rate for each layer. Our topology improves the situation by making training uniform among the deeper layers, although the shallowest layer still trains more-quickly than the deeper layers.

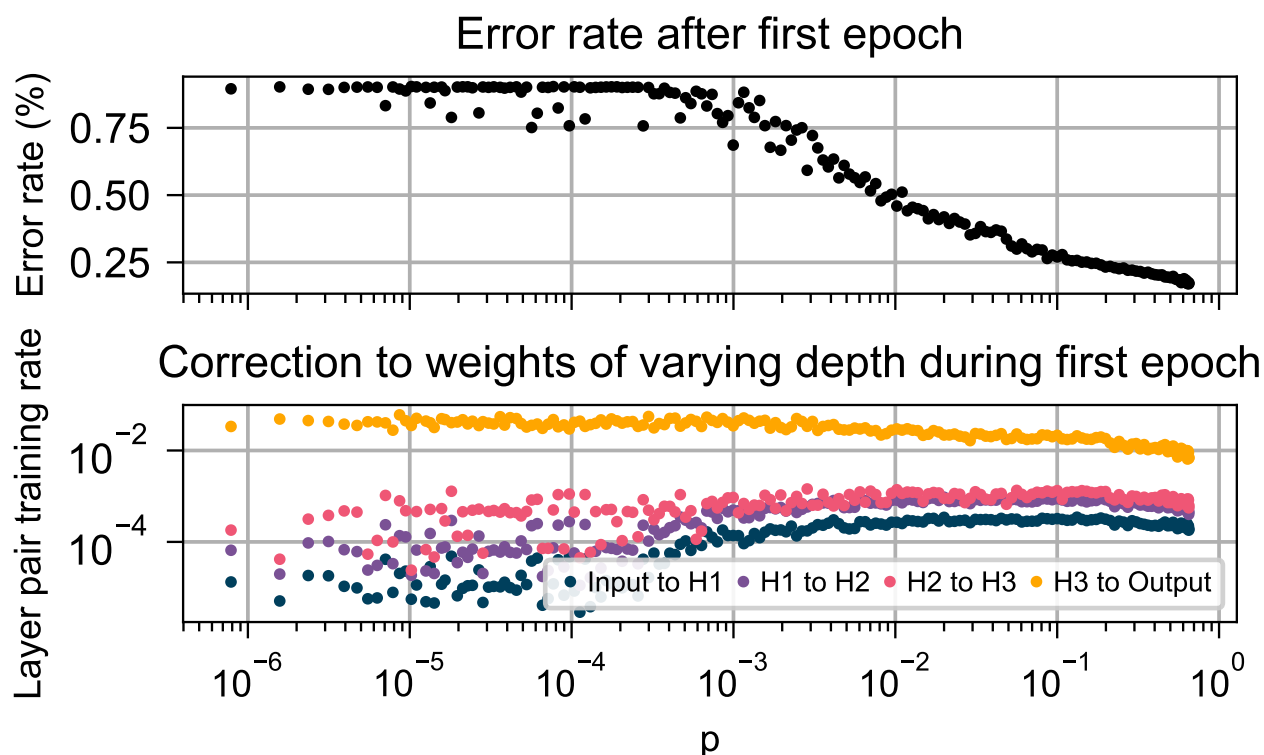


Figure 5. Behavior of our network (section 3.3) with varying p , during the first epoch of training. (top) The training error after one epoch. (bottom) Root-mean-square correction to weights in different layers during the first epoch. Observe that as p is increased, the error rate decreases and the root-mean-square corrections to each layer become more-uniform.

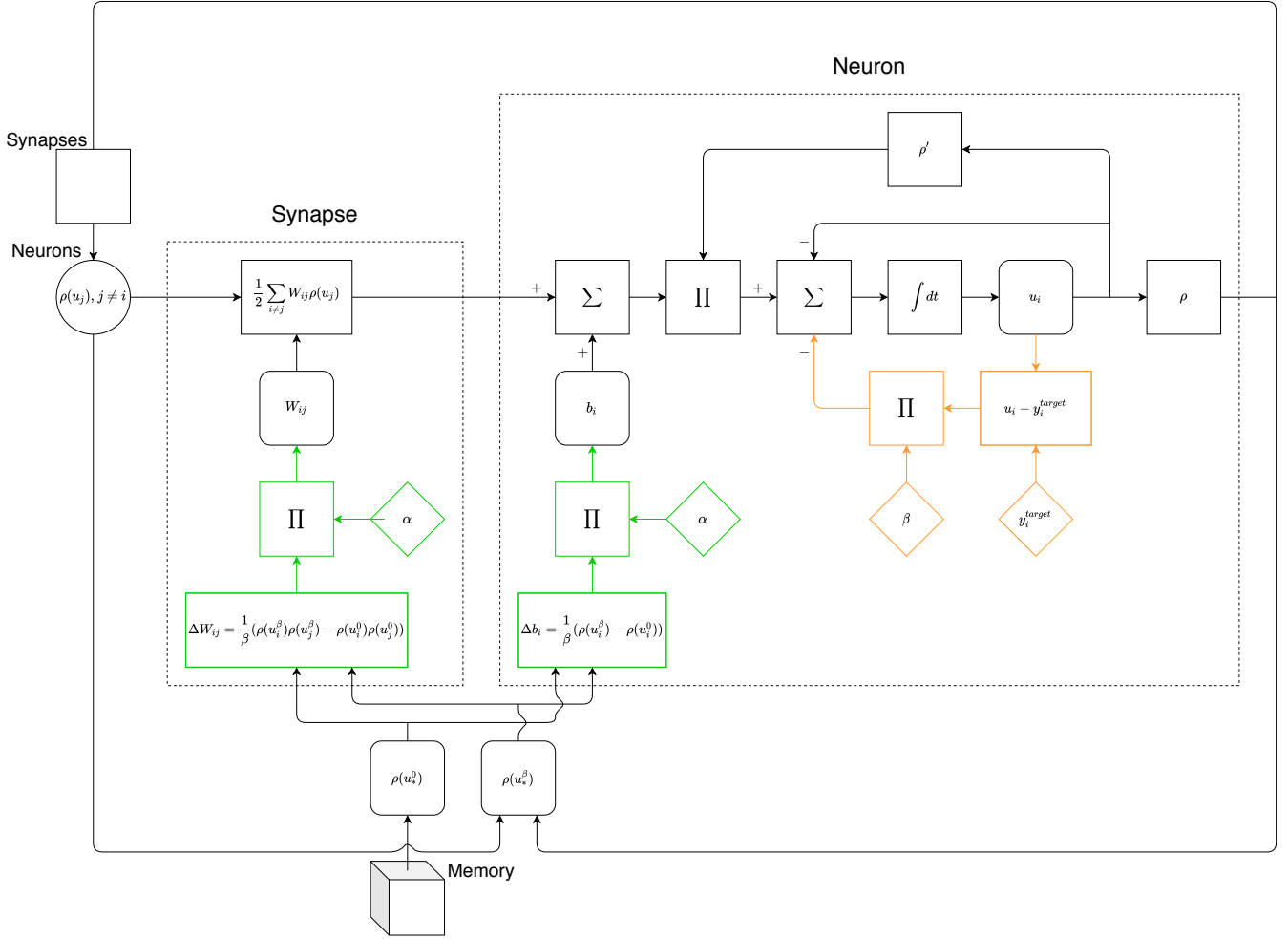


Figure 6. Illustration of the functionality needed to implement equilibrium propagation in hardware. Black lines denote functionality needed in the free phase. Green lines denote functionality to correct parameters. Orange lines denote functionality needed only by output neurons, that is unique to the weakly-clamped phase. There is no functionality unique to the weakly-clamped phase that is needed by all neurons.

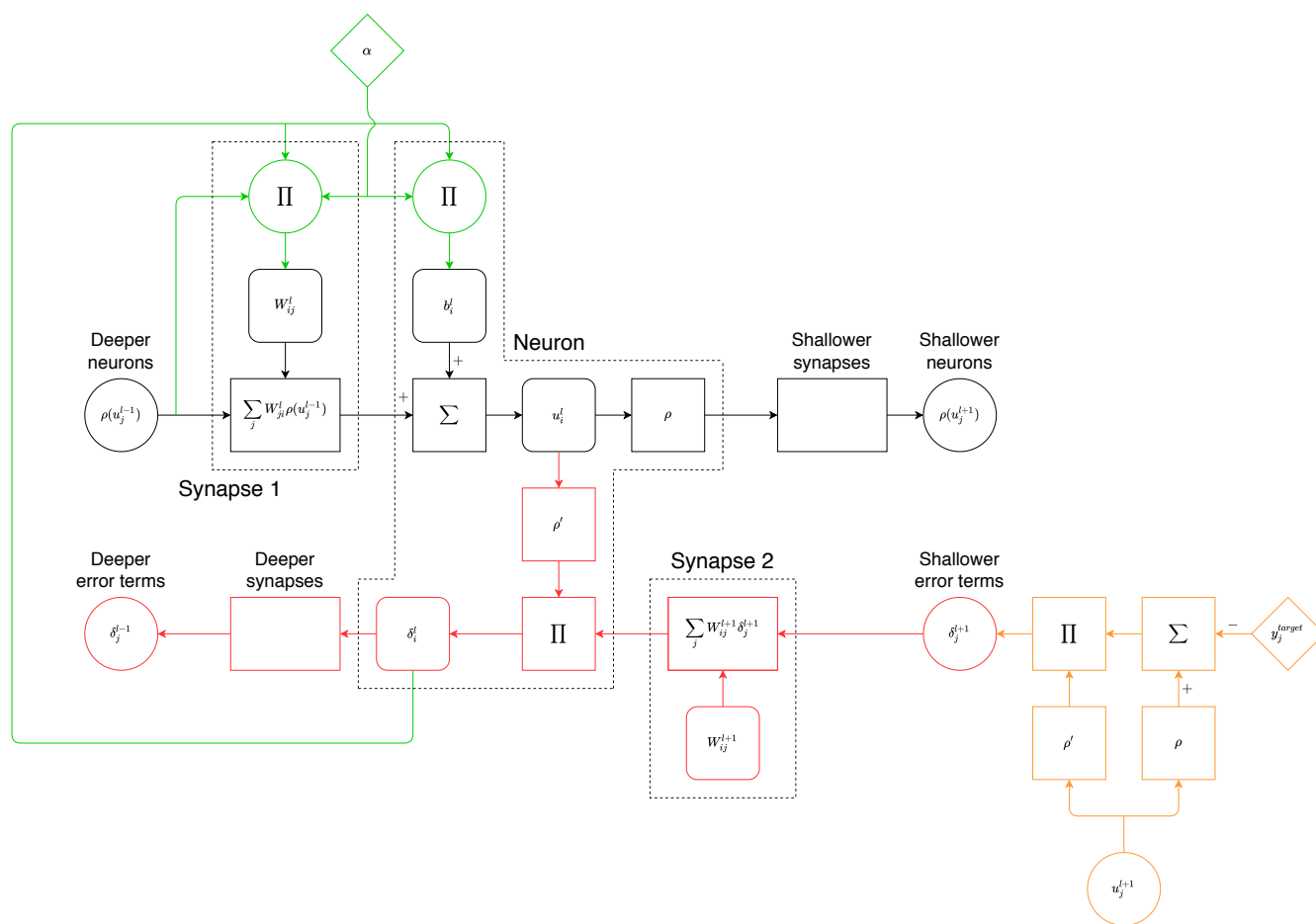


Figure 7. Illustration of the functionality needed to implement backpropagation in hardware. Black lines denote functionality needed in the forwards phase. Green lines denote functionality to correct parameters. Red lines denote functionality unique to the backwards phase that is needed by all neurons. Orange lines denote functionality needed only by output neurons, that is unique to the backwards phase.

TABLES

	Backpropagation	Equilibrium Propagation
Memory	Space to store activation and error term for each neuron	Space to store free and weakly-clamped activations for each neuron
Nonlinear activation function	Yes	Yes
Derivative of nonlinear activation function	Yes	Yes
Number of distinct computations	2 - computations during forwards and backwards phases are distinct	≈ 1 - hidden neurons perform same computation in both phases. Output neurons perform a similar but modified version of the same computation.
Types of connections	Unidirectional to transmit activation to shallower neighbors and error to deeper neighbors	Bidirectional to each neighbor
Correction computation	Corrections require dedicated circuitry unique from that implementing propagation	Corrections require dedicated circuitry unique from that implementing evolution
Order of computations	Forwards propagation phase where layers are computed from deepest to shallowest; backwards propagation phase where layers are computed from shallowest to deepest; parameter update phase	Free phase where all neurons evolve simultaneously; weakly-clamped phase where all neurons evolve simultaneously; parameter update phase

Table 1. Comparison of the capabilities a hardware neuron would need in order to implement backpropagation and equilibrium propagation.